Scientific Inquiry and Review (SIR)
Volume 8 Issue 3, 2024
ISSN$_{(P)}$: 2521-2427, ISSN$_{(E)}$: 2521-2435
Homepage: https://journals.umt.edu.pk/index.php/SIR

Article QR

Title:	**Comparison of Adams-Bashforth-Moulton and Dormand-Prince Methods in Lengyel-Epstein Reaction Model Forming Zinc Oxide Nanostructures**
Author (s):	Kaniz Fatima[1], Sarwat Ishaque[2], Humaira Ahmed[3], and Basit Ali[4]
Affiliation (s):	[1]Department of Humanities and Social Sciences, Bahria University Karachi Campus, Pakistan [2]KASB Institute of Technology, Karachi, Pakistan [3]Sir Syed University of Engineering and Technology, Karachi, Pakistan [4]Department of Electrical Engineering, Bahria University Karachi Campus, Pakistan
DOI:	https://doi.org/10.32350/sir.83.04
History:	Received: February, 02, 2024, Revised: 24 May, 2024, Accepted: June 02, 2024, Published: September 26, 2024
Citation:	Fatima K, Ishaque S, Ahmed H, Ali B. Comparison of Adams-Bashforth-Moulton and Dormand-Prince methods in Lengyel-Epstein reaction model forming Zinc Oxide nanostructures. *Sci Inq Rev.* 2024;8(3):88–101. https://doi.org/10.32350/sir.83.04
Copyright:	© The Authors
Licensing:	This article is open access and is distributed under the terms of Creative Commons Attribution 4.0 International License
Conflict of Interest:	Author(s) declared no conflict of interest

A publication of
The School of Science
University of Management and Technology, Lahore, Pakistan

Comparison of Adams-Bashforth-Moulton and Dormand-Prince Methods in Lengyel-Epstein Reaction Model Forming Zinc Oxide Nanostructures

Kaniz Fatima[1 *], Sarwat Ishaque[2], Humaira Ahmed[3], and Basit Ali[4]

[1]Department of Humanities and Social Sciences, Bahria University Karachi campus, Pakistan
[2]Department of CS and Quantitative, KASBIT, Karachi, Pakistan
[3]Department of Mathematics and Sciences, Sir Syed University of Engineering and Technology, Karachi, Pakistan
[4]Department of Electrical Engineering, Bahria University Karachi Campus, Pakistan

ABSTRACT

This study adopts a numerical approach in the Lengyel-Epstein reaction model for forming zinc oxide (ZnO) nanostructures. It aims to determine the optimal approximation technique to analyze the growth of ion concentrations in ZnO nanostructures. For this purpose, ordinary differential equations are developed using the Dormand-Prince method in the Lengyel-Epstein reaction model. The results obtained from this technique are compared with the results obtained from the Adams-Bashforth-Moulton (ABM) method. After a comparative analysis of both methods, the results showed that the ABM method performs better than the Dormand-Prince method. The accuracy and stability of the ABM method are higher than those of the Dormand-Prince method. Furthermore, error analysis for both methods confirms that the results obtained from the former are more optimized. Moreover, this method also validates the results obtained from the experimental procedure by using the aqueous chemical growth (ACG) method to form the nanostructures of ZnO.

Keywords: Adams-Bashforth-Moulton (ABM) method, aqueous chemical growth, Dormand-Prince method, Lengyel-Epstein reaction model, ordinary differential equations, zinc oxide (ZnO) nanostructures

1. INTRODUCTION

Zinc oxide (ZnO) is an inorganic compound that has outstanding applications in the world of technology. Naturally, it is white in color and found in powder form. It is not soluble in water but is easily soluble in

* Corresponding Author: kanizfatima.bukc@bahria.edu.pk

diluted acids and bases [1]. Furthermore, it is a good conductor of electricity and also characterized by strong absorption of ultraviolet rays [2]. Due to these properties, ZnO can be used to make electronic, photovoltaic, and biomedical devices [3]. Having the property of absorbing UV rays, it can be used also in making skin lotions, sunblock, and wound healing ointments [4]. ZnO is an antimicrobial compound, so it can be used in products that reduce acne and treat other infections related to the skin [5].

The higher biocompatibility of this compound makes it favorable for the drug delivery system. Hence, it is also certified by the US Food and Drug Administration (FDA) [6]. Some more applications include in fields Turing patterns in human beings and animals, drug delivery, morphogenesis, and tissue development [7]. Further, ZnO has a wide range of applications in the medical field due to its antibacterial properties. It is used in hygiene products because it helps to prevent the growth of bacteria and increases the lifespan of the products [8]. It also helps in the treatment of diabetic patients because it contains zinc which has the ability to normalize the level of insulin [9].

The binding energy of ZnO is very high at room temperature, that is, around 60 meV, as compared to other semiconductors [10]. Due to this fact, electron mobility is quite high, resulting in its amazing electrical properties [11]. This is very important for the production of electronic and optoelectronic devices [12]. It can also be used in light emitting devices, sensors, and displays because ZnO nanoparticles are known for their room temperature luminescence [13]. They are also distinguished by their extraordinarily small size, typically less than 100 nm, which imparts them with distinctive physical and chemical properties that set them apart from other metal oxides [14]. This nanoparticle dimension is important because it significantly increases the surface area to volume ratio, increasing their reactivity, mechanical strength, and electronic properties [15]. These characteristics make ZnO nanoparticles indispensable in a broad group of industries. ZnO also has antifungal property, so it can be used in the paint industry because it makes the coatings of paints more durable and its nanoparticles contribute to better weather resistance [16]. Another significant usage of ZnO is in rubber and plastic industries where it acts as a reinforcing agent to increase the strength of utensils [17].

A wide range of ZnO nanostructures can be formed by using the method of aqueous chemical growth (ACG) [18]. This method is simple and

effective and can be performed at room temperature. In this method, there is specific control over the morphology and size of ZnO nanostructures, including nanowires, nanorods, nanoflexes, nanosphere, nanoneedles, and nanotubes. Due to this fact, the ACG method is also preferred for the large scale production of ZnO [19]. The formation of ZnO can be analyzed by using mathematical modelling. Lengyel-Epstein reaction model helps to predict the concentrations of zinc ions Zn^{2+} and hydroxyl ions OH^{-} to form ZnO nanostructures [20] . To solve differential equations in this model, different numerical techniques can be used. In previous studies, Euler's method, fourth order Runge Kutta method, and Adams-Bashforth-Moulton (ABM) method were used to solve the differential equations of this model. The ABM method surpassed the other methods and provided more accurate results. In this study, a different numerical technique is used to approximate the concentrations of OH^{-} and Zn^{2+}. The Lengyel-Epstein reaction model is modelled by using the Dormand-Prince method for the first time in this study.

Dormand-Prince method belongs to the Runge Kutta method's family [21]. To get the numerical solutions of differential equations, it involves both fourth and fifth order Runge Kutta methods [22]. This method constitutes the ultimate option to solve differential equations due to its high level of accuracy. It controls the step size based on error estimation and optimizes the efficiency of computations. Some of the implantations are reported in [23]. In this paper, a comparative analysis is made between the results of the Dormand-Prince method and the Adams-Bashforth-Moulton method. Both methods were used in Lengyel-Epstein reaction model to visualize the concentrations of OH^{-} and Zn^{2+}. The error analysis of both the methods showed that the ABM method delivers more accurate and stable results than the Dormand-Prince method for this model.

2. EXPERIMENTAL PROCEDURE

In a controlled environment, a large amount of ZnO nanoparticles can be produced by using the aqueous chemical growth (ACG) method. Starting from the initial process, the substrate is coated with gold to minimize the contaminations. Before starting the synthesis, the substrate is immersed in a low concentration hydrofluoric acid solution. This is followed by using the spin coating technique, that is, using acetone for cleaning and drying at room temperature with the help of nitrogen gas. The solution of zinc acetate dihydrate is applied to the substrate, which is rotated at 4500 rpm. This

procedure is repeated multiple times till the solution is applied completely to the substrate. After the complete application of the solution, the substrate is heated to 70°C to stabilize the solution [24]. Meanwhile, another solution is prepared in 250 ml of deionized water by fusing zinc nitrate and hexamethylenetetramine in a 1:1 ratio. The pre-coated substrate is then immersed in this prepared solution, placed in a container, and heated in an oven for 7 hours at 100°C. Afterward, the oven is turned off and the container is allowed to cool for 30 minutes. The substrate is then detached from the container, revealing a layer of ZnO nanorods.

For the formation of ZnO nanowires, adjusting the pH of the solution with 25% ammonia solution increases the diversity of the synthesized nanostructures [25]. The production of ZnO requires two ions, namely zinc ions Zn^{2+} and hydroxyl ions OH^-.

Zn^{2+} is produced from the separation of zinc nitrate in water.

$$Zn(NO_3)_2.6H_2O + 6H_2O \rightarrow Zn^{+2} + 2NO_3^-$$

OH^- is produced after the hydrothermal breakdown of HMT.

$$(CH_2)_6N_4 + 6H_2O \rightarrow 6HCHO + 4NH_3$$

ZnO is produced after the deposition of both zinc ions Zn^{2+} and hydroxyl ions OH^-

$$2OH^- + Zn^{+2} \rightarrow Zn(OH)_2$$

$$Zn(OH)_2 \rightarrow ZnO\ (s)\ +\ H_2O$$

3. MATHEMATICAL MODEL

A mathematical model may be used to demonstrate the production rate of the zinc ion Zn^{+2} and hydroxide ion OH^- concentrations needed for the production of ZnO. The Lengyel-Epstein reaction model is applied for this purpose. The ABM method is implemented as a numerical technique in this model to approximate the results in previous studies [26]. Moreover, this study uses the Dormand-Prince method to estimate the growth of zinc and hydroxyl ions. The following equations are used in the modelling of Lengyel-Epstein reaction. The differential equations are formulated based on the theoretical framework.

$$NH_3 + H_2O \rightarrow NH_4^+ + OH^- \quad (1)$$

$$Zn(NO_3)_2.6H_2O + 6H_2O \rightarrow Zn^{+2} + 2NO_3^- \quad (2)$$

$$2OH^- + Zn^{+2} \rightarrow ZnO + H_2O \quad (3)$$

The differential equations describe the dynamics of the concentrations of hydrogen ion OH^- and zinc ion Zn^{+2}, represented by x and y, respectively.

These equations are as follows:

$$\frac{dx}{dt} = u(x,y) = \alpha - x - 4\left(\frac{xy}{(1+x^2)}\right) \quad (4)$$

$$\frac{dy}{dt} = v(x,y) = \beta x\left(1 - \frac{y}{(1+x^2)}\right) \quad (5)$$

The parameters α and β play important roles in determining the behavior of the system. The condition $\beta > \frac{3\alpha}{5} - \frac{25}{\alpha}$ is used to evaluate the concentrations of OH^- and Zn^{2+} in steady state. It was also shown experimentally that the growth of ZnO reaches a steady state after a certain time and shows a linear behavior [26] . Mathematically, to solve these differential equations, several methods can be applied to approximate the concentrations of OH^- and Zn^{2+} [27]. To find the approximate solutions, the Dormand-Prince method is used. This method is an iterative method and provides good estimated values of the concentrations of OH^- and Zn^{2+}. Furthermore, the results of the Dormand-Prince method are compared with the ABM method to study the growth kinematics in ZnO nanostructures.

3.1. Adams-Bashforth-Moulton (ABM) Method

To solve the system of differential equations, the ABM method is a useful numerical approach. This method is implemented to increase the computational accuracy of the Lengyel-Epstein reaction model which is used to determine the growth of ZnO nanostructures. This method consists of two steps, namely predictor and corrector steps. To find out the values of the next iteration, x_{pred} and y_{pred} are calculated. The following procedure is to be followed for the implementation of this method:

$$x_{pred} = x_i + \frac{\Delta t}{24}(55u_i - 59u_{i-1} + 37u_{i-2} - 9u_{i-3}) \quad (6)$$

$$y_{pred} = y_i + \frac{\Delta t}{24}(55v_i - 59v_{i-1} + 37v_{i-2} - 9v_{i-3}) \quad (7)$$

Here, u_i and v_i represent the predicted values of the differential equations at time t_i. The next step is the corrector step to obtain more

refined predicted values of x and y by using the previous values of x_{pred} and y_{pred}.

$$x_{i+1} = x_i + \frac{\Delta t}{24}\left(9u_{pred} + 19u_i - 5u_{i-1} + u_{i-2}\right) \quad (8)$$

$$y_{i+1} = y_i + \frac{\Delta t}{24}\left(9v_{pred} + 19v_i - 5v_{i-1} + v_{i-2}\right) \quad (9)$$

The integration method continues iteratively over the specified time period, continually refining the values of x and y by applying the predicted and corrected estimates.

3.2. Dormand-Prince Method

In numerical analysis, the Dormand-Prince method is an iterative technique known for its unique ability to achieve high accuracy and efficiency in solving ordinary differential equations. This method is an important member of the Runge Kutta family and is distinguished for its adaptive step size control. It employs specific coefficients that calculate intermediary stages which ensure high order accuracy, usually fourth or fifth. The function estimation at each stage is determined by using the Butcher tableau of the Dormand-Prince method as follows:

$$k_1 = hf(x_i, y_i) \quad (10)$$

$$k_2 = hf\left(x_i + \frac{1}{5}h,\ y_i + \frac{1}{5}k_1\right) \quad (11)$$

$$k_3 = hf\left(x_i + \frac{3}{10}h,\ y_i + \frac{3}{40}k_1 + \frac{9}{40}k_2\right) \quad (12)$$

$$k_4 = hf\left(x_i + \frac{4}{5}h,\ y_i + \frac{44}{45}k_1 - \frac{56}{15}k_2 + \frac{32}{9}k_3\right) \quad (13)$$

$$k_5 = hf\left(x_i + \frac{8}{9}h,\ y_i + \frac{19372}{6561}k_1 - \frac{25360}{2187}k_2 + \frac{64448}{6561}k_3 - \frac{212}{729}k_4\right) \quad (14)$$

$$k_6 = hf\left(x_i + h,\ y_i + \frac{9017}{3168}k_1 - \frac{355}{33}k_2 + \frac{46732}{5247}k_3 + \frac{49}{176}k_4 - \frac{5103}{18656}k_5\right) \quad (15)$$

For the next step, the value of y_{k+1} is computed as follows:

$$y_{k+1} = y_k + \frac{35}{384}k_1 + \frac{500}{1113}k_3 + \frac{125}{192}k_4 - \frac{2187}{6784}k_5 + \frac{11}{84}k_6 \quad (16)$$

This iterative method increases the accuracy of the results while also improving computational efficiency.

4. RESULTS AND DISCUSSION

Figure 1 illustrates a detailed description of the concentrations of OH^{-} and Zn^{+2} as determined by the exact solution of the obtained differential equations of the model. The graph highlights a significant point where the OH^{-} concentration drops to its lowest value of 0.38080 at about 1.18658 hours. Simultaneously, the concentration of Zn^{+2} exhibits a maximum point, getting the highest value of 1.30732 at about 0.41048 hours.

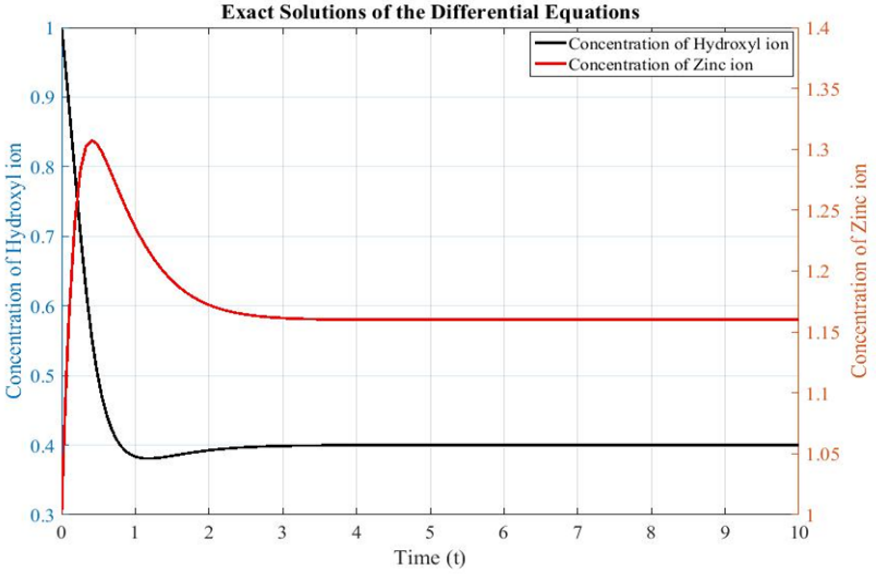

Figure 1. Concentrations of OH^{-} and Zn^{+2} for the Exact Solution

Similarly, Figure 2 depicts the concentrations of OH^{-} and Zn^{+2} as determined by using the ABM method to solve the differential equations. The minimum value of OH^{-} concentration is 0.3806 at 1.18658 hours and the maximum value of Zn^{+2} concentration is 1.30886 at time 0.41048 hours. These values are close enough to the exact values which proves that this method shows a good accuracy level and exhibits minimum error.

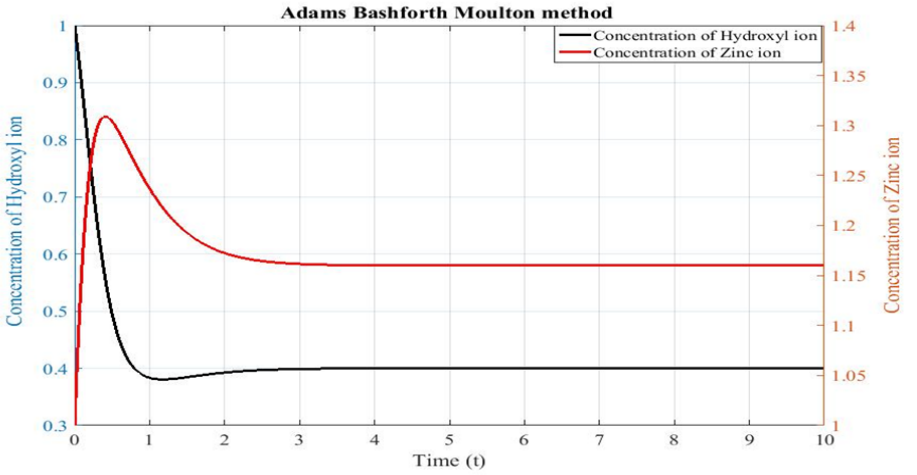

Figure 2. Concentrations of OH^- and Zn^(+2) for the ABM Method

Figure 3 shows the OH^- and Zn^{+2} concentrations determined by the Dormand-Prince method. The minimum value of OH^- concentration is 0.37939 at 1.18658 hours and the maximum value of Zn^{+2} concentration is 1.31471 at time 0.41048 hours. These values are also close to the exact solutions but show less accuracy than the values obtained by the ABM method.

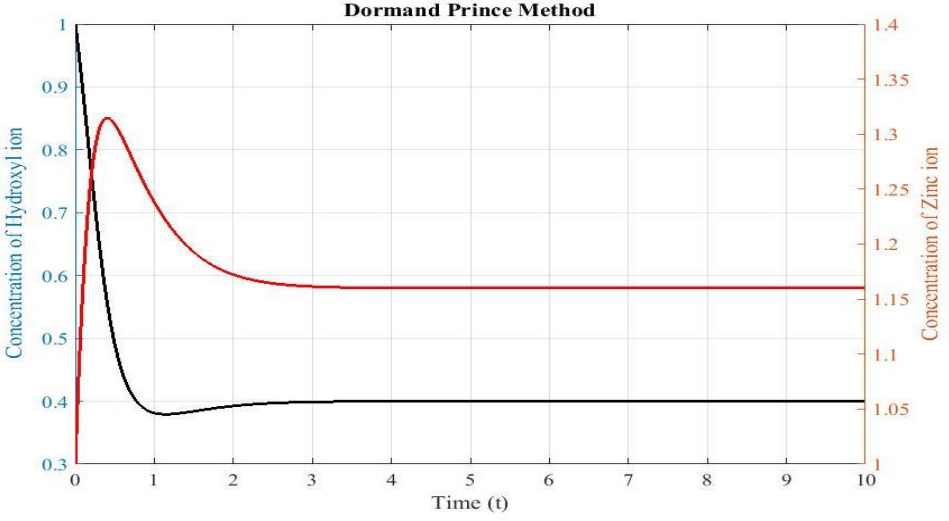

Figure 3. Concentrations of OH^- and Zn^{+2} for the Dormand-Prince Method

The comparative analysis of $OH^{-}$and Zn^{+2} concentrations using the ABM method and Dormand-Prince method is shown in Table 1. The results show a thorough analysis of the critical values given by both methods. The values obtained from the ABM method are better than the values obtained by the Dormand-Prince method, when compared with the exact results. Although the prediction of $OH^{-}$and Zn^{+2} concentrations using the Dormand-Prince method is good; still, when it is compared with the ABM method, the estimation of the latter is more accurate.

Table 1. Concentrations of OH^{-} and Zn^{+2} for Numerical Methods

Method	Concentrations of OH^{-}	Concentrations of Zn^{+2}
	For t =1.18658	For t =0.41048
Adams-Bashforth-Moulton	0.38060	1.30886
Dormand-Prince	0.37939	1.31471

4.1. Error Analysis

The estimation of OH^{-} and Zn^{+2} concentrations from both the methods give approximate results to their exact solution but also show some differences. The result of OH^{-} concentration at t = 1.18658 hours obtained via the ABM method is more accurate than the result obtained by using the Dormand-Prince method. Similarly, the result of Zn^{+2} concentration at t = 0.41048 hours obtained via the ABM method is more reliable. The error analysis of both the methods is also conducted. The error from the Dormand-Prince method at t=1.18658 hours is 0.370% for OH^{-} concentration and 0.565% at t= 0.41048 hours for Zn^{+2} concentration, as shown in Table 2.

Table 2. Error Analysis of OH^{-} and Zn^{+2} Concentrations

Method	Concentrations of OH^{-}	Concentrations of Zn^{+2}
	For t=1.18658	For t =0.41048
Adams-Bashforth-Moulton	0.053%	0.118%
Dormand-Prince	0.370%	0.565%

Figure 4 shows the comparative error analysis of both the methods. This comparison highlights the importance of selecting the suitable numerical approach for the Lengyel-Epstein reaction model to ensure accuracy and efficiency.

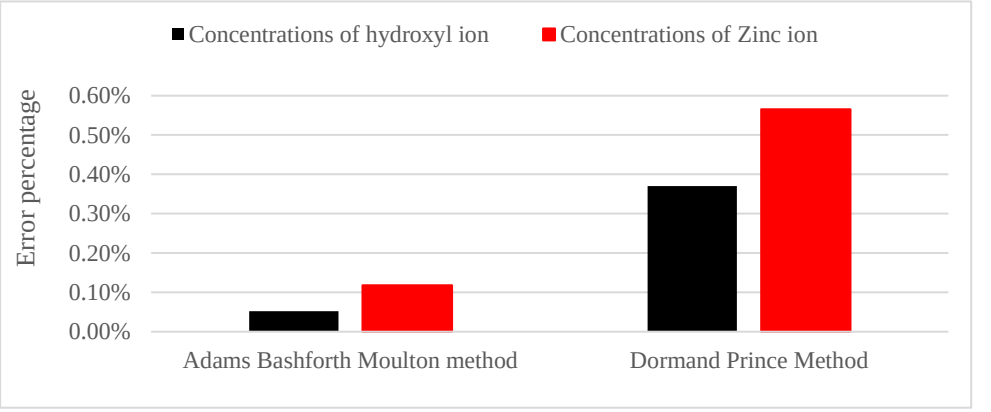

Figure 4. Error Estimation of OH^{-} and Zn^{+2} Concentrations

4.2. Conclusion

In this study, two different numerical approaches are compared. The results depict that the ABM method shows a higher accuracy and stability than the Dormand-Prince method. The values obtained from the ABM are very close to the exact solution of differential equations and bear little error. Meanwhile, the Dormand-Prince method significantly differs from the exact solution. Although this method is effective and provides better approximation than many other methods, the error estimation of this method is larger than the ABM method. So, to estimate the concentrations with the help of the Lengyel-Epstein reaction model, the use of the ABM method is more advantageous than the other methods. To conclude, ABM outperforms the Dormand-Prince method, which is evident from the numerical results presented. The same is also confirmed by error analysis so presented.

CONFLICT OF INTEREST

The authors of the manuscript have no financial or non-financial conflict of interest in the subject matter or materials discussed in this manuscript.

DATA AVALIABILITY STATEMENT

Data availability is not applicable as no new data was created.

FUNDING DETAILS

No funding has been received for this research.

REFERENCES

1. Siddiqi KS, Rahman A, Tajuddin, Husen A. Properties of zinc oxide nanoparticles and their activity against microbes. *Nanoscale Res Lett*. 2018;13:e141. https://doi.org/10.1186/s11671-018-2532-3
2. Ali B, Khan AA. Real-time distribution system analysis and load management algorithm for minimizing harmonics. *Roman J Tech Sci*. 2021;66(4):237–242.
3. Ali B, Khan AA, Ali A, Maqsood M, Nisha R. Power loss reduction of distribution network in densely industrialized coastal belt by development of hydrophobic coating applying accelerated aging for ceramic insulator. *ASEAN Eng J*. 2022;12(1):111–117. https://doi.org/10.11113/aej.v12.17209
4. Fatima K, Khan A, Hussain M. Mathematical modelling of reaction kinematics of one dimensional Zinc oxide nanostructures. *NED Univ J Res*. 2018;15(4):117–122.
5. Holmes AM, Song Z, Moghimi HR, Roberts MS. Relative penetration of zinc oxide and zinc ions into human skin after application of different zinc oxide formulations. *ACS Nano*. 2016;10(2):1810–1819. https://doi.org/10.1021/acsnano.5b04148
6. Mishra PK, Mishra H, Ekielski A, Talegaonkar S, Vaidya B. Zinc oxide nanoparticles: a promising nanomaterial for biomedical applications. *Drug Discov Today*. 2017;22(12):1825–1834. https://doi.org/10.1016/j.drudis.2017.08.006
7. Sabir S, Arshad M, Chaudhari SK. Zinc oxide nanoparticles for revolutionizing agriculture: synthesis and applications. *Sci World J*. 2014;2014(1):e925494. https://doi.org/10.1155/2014/925494
8. Jiang J, Pi J, Cai J. The advancing of zinc oxide nanoparticles for biomedical applications. *Bioinorg Chem Appl*. 2018;2018(1):e1062562. https://doi.org/10.1155/2018/1062562
9. Tang E, Cheng G, Ma X, Pang X, Zhao Q. Surface modification of zinc oxide nanoparticle by PMAA and its dispersion in aqueous system. *Appl*

Surf Sci. 2006;252(14):5227–5232. https://doi.org/10.1016/j.apsusc.2005.08.004

10. Kulkarni SS, Shirsat MD. Optical and structural properties of zinc oxide nanoparticles. *Int J Adv Res Phys Sci*. 2015;2(1):14–18.
11. Gaspar D, Pereira L, Gehrke K, Galler B, Fortunato E, Martins R. High mobility hydrogenated zinc oxide thin films. *Sol Energy Mater Sol Cells*. 2017;163:255–262. https://doi.org/10.1016/j.solmat.2017.01.030
12. Ding M, Guo Z, Zhou L, et al. One-dimensional zinc oxide nanomaterials for application in high-performance advanced optoelectronic devices. *Crystals*. 2018;8(5):e223. https://doi.org/10.3390/cryst8050223
13. Rahman F. Zinc oxide light-emitting diodes: a review. *Opt Eng*. 2019;58(1):010901–010901. https://doi.org/10.1117/1.OE.58.1.010901
14. Jitianu M, Goia DV. Zinc oxide colloids with controlled size, shape, and structure. *J Colloid Interface Sci*. 2007;309(1):78–85. https://doi.org/10.1016/j.jcis.2006.12.020
15. Li D, Haneda H. Morphologies of zinc oxide particles and their effects on photocatalysis. *Chemosphere*. 2003;51(2):129–137. https://doi.org/10.1016/s0045-6535(02)00787-7
16. Moezzi A, McDonagh AM, Cortie MB. Zinc oxide particles: Synthesis, properties and applications. *Chem Eng J*. 2012;185:1–22. https://doi.org/10.1016/j.cej.2012.01.076
17. Begum PS, Joseph R, Yusuff KM. Preparation of nano zinc oxide, its characterization and use in natural rubber. *Prog Rubber Plast Recycl Technol*. 2008;24(2):141–152. https://doi.org/10.1177/147776060802400204
18. Osman DAM, Mustafa MA. Synthesis and characterization of zinc oxide nanoparticles using zinc acetate dihydrate and sodium hydroxide. *J Nanosci Nanoeng*. 2015;1(4):248–251.
19. Fatima K, Ali B, Mahnoor. Implementation of lengyel-epstein reaction model for zinc Oxide (ZnO) nanostructures by comparing euler and fourth-order Runge–Kutta (RK) methods. *Sci Inq Rev*. 2022;6(1):23–33. https://doi.org/10.32350/sir.61.02

20. Mammah SL, Opara FE, Sigalo FB, Ezugwu SC, Ezema FI. Effect of concentration on the optical and solid state properties of ZnO thin films deposited by aqueous chemical growth (ACG) method. *J Mod Phys*. 2012;3(10):1516–1522.

21. Dormand JR, Prince PJ. A family of embedded Runge-Kutta formulae. *J Comput Appl Math*. 1980;6(1):19–26. https://doi.org/10.1016/0771-050X(80)90013-3

22. Ang TK, Hamzah A, Shamsidah N. *Solving Ordinary Differential Equations by the Dormand Prince Method*. Penerbit UTHM; 2018.

23. Shaikh WA, Keerio MU, Shaikh AG, Naz L, Sheikh AH. Higher order runge-kutta method for solving system of ordinary differential equations using MS excel. *Quaid-E-Awam Univ Res J Eng Sci Technol Nawabshah*. 2021;19:36–41. https://doi.org/10.52584/qrj.1902.06

24. Lee CY, Wang J, Chou Y, et al. White-light electroluminescence from ZnO nanorods/polyfluorene by solution-based growth. *Nanotechnology*. 2009;20(42):e425202. https://doi.org/10.1088/0957-4484/20/42/425202

25. Chicone C. *Mathematical modeling and chemical kinetics*. University of Missouri; 2010. https://www.simiode.org/resources/7215/download/2010-Chicone-MathModelingANDChemicalKinetics.pdf

26. Mishra YK, Modi G, Cretu V, et al. Direct growth of freestanding ZnO tetrapod networks for multifunctional applications in photocatalysis, UV photodetection, and gas sensing. *ACS Appl Mater Interfaces*. 2015;7(26):14303–14316. https://doi.org/10.1021/acsami.5b02816

27. Caetano BL, Santilli CV, Meneau F, Briois V, Pulcinelli SH. In situ and simultaneous UV- vis/SAXS and UV- vis/XAFS time-resolved monitoring of ZnO quantum dots formation and growth. *J Phys Chem C*. 2011;115(11):4404–4412. https://doi.org/10.1021/jp109585t